Annex 5

General Discussion

In this annex a general and comparative discussion of the effects of FM-AFM exchange interactions induced by ball milling in Co + NiO, $SmCo_5$ + NiO and $SmCo_5$ + CoO will be given. The aim of this annex is to emphasize the differences in the structural and magnetic behaviors of the three systems studied and also in the processing routes that have been used to induce the FM-AFM coupling in each of them.

In annex 3 it has been shown that ball milling of FM (Co or $SmCo_5$) with AFM (NiO or CoO) powders creates a microstructure consisting of composites of several μm in which the FM grains are embedded in an AFM or PM (in CoO) matrix [1-4]. Within these composites many interfaces are created between the FM and the AFM grains, where FM-AFM exchange interactions mainly take place. The amount of FM-AFM interfaces is expected to be larger for larger FM-AFM composites. To study this effect the 20 h ball milled Co-NiO composites were separated into different particle sizes, $\boldsymbol{F}$, by means of different sieves and the influence of the particle size on the coercivity enhancement was analyzed [1]. From the morphological description given in annex 3 it is clear that the largest particles will have a larger FM-AFM interface area, since they are agglomerates of Co grains embedded in the NiO matrix, while the smaller particles are mainly Co or NiO grains still not soldered together. In table 5.1 the dependence of H_C on the particle size, before and after a field cooling process from T_{ANN} = 600 K, is given.

Size (μm)	$\boldsymbol{F} > 100$	$50 < \boldsymbol{F} < 100$	$25 < \boldsymbol{F} < 50$	$\boldsymbol{F} < 25$
H_C (± 3 Oe), as milled	303	306	301	291
H_C (± 3 Oe), field-cooled	353	355	343	330

Table 5.1. Dependence of the coercivity, H_C, on the particle size, $\boldsymbol{F}$, for Co ball milled with NiO for 20 h in a weight ratio of 1:1 and field cooled from T_{ANN} = 600 K in H = 5 kOe

The coercivity of as-milled powders is similar for all sizes and only slightly lower for the smallest particles. However, after annealing at T_{ANN} = 600 K for 0.5 h and field cooling to room temperature, H_C is found to depend markedly on $\boldsymbol{F}$. The highest values of H_C were

obtained for $\boldsymbol{F}$ > 50 μm, as expected from their microstructure, i.e. fine Co lamellae embedded in the NiO matrix.

Although in the three systems studied (i.e. Co + NiO, $SmCo_5$ + NiO and $SmCo_5$ + CoO) the microstructure of as-milled powders is very similar, the magnetic properties vary a lot depending on the FM and the AFM that are being processed. For instance, when milling with NiO, the effects of these interactions can be observed at room temperature since the Néel temperature of NiO is above room temperature (T_N (NiO) = 590 K). On the contrary, as has been described in annex 4, for $SmCo_5$ + CoO, a coercivity enhancement (with respect to the maximum of $SmCo_5$ milled alone) is only observed after field cooling to below room temperature, since T_N (CoO) = 290 K [5].

The different structural and magnetic behaviors of Co and $SmCo_5$ during ball milling or heat treatments, make it also necessary to adapt in each case the processing route to optimize the effects of the coupling. As has been described in annex 1, a field cooling process from above T_N is usually required in order to induce FM-AFM exchange interactions [6]. Therefore as-milled Co + NiO composites were annealed and field cooled from above T_N and, as expected, this resulted in an enhancement of the room temperature coercivity and a shift of the hysteresis loop. Furthermore, since no significant structural changes occur in Co when heated at intermediate temperatures (i.e. from room temperature to T_N), several heating/cooling experiments could be carried out in this system to study the thermal stability of the FM-AFM coupling (see sections 4.1.5 and 4.1.6). However, in $SmCo_5$ + AFM (NiO or CoO) powders, heating results in a rapid deterioration of the hard FM properties, mainly due to the formation, at intermediate temperatures, of non-magnetic or softer phases (Sm_2Co_7 or Sm_2Co_{17}), which leads to a loss of the magnetic anisotropy [7]. Moreover, annealing of $SmCo_5$ + NiO has also shown to result in Sm oxidation, since Sm is more reactive to oxygen than Ni or Co. Therefore, in $SmCo_5$ + NiO, the induction of FM-AFM exchange interactions by heating and field cooling the as-milled powders seems very difficult if not impossible.

Nevertheless, as has been discussed in annex 4 (see figure 4.16), a comparative study of the milling time dependences of H_C for $SmCo_5$ milled alone, with CoO and with NiO (i.e. an enhancement of H_C is observed in $SmCo_5$ + NiO with respect to $SmCo_5$ alone or $SmCo_5$ + CoO) reveals that, to some extent, FM-AFM exchange interactions are likely to be induced during the milling of $SmCo_5$ with AFM NiO powders. Actually, several factors have to be taken into account in order to explain the milling time dependence of H_C in ball milled $SmCo_5$ + CoO and $SmCo_5$ + NiO powders. As has been noted in annex 4, H_C increases for short milling times in $SmCo_5$ either when it is milled alone or with NiO or CoO. This can be mainly attributed to the particle size reduction associated with the milling process. It should be recalled that the unmilled $SmCo_5$ particles are several μm in size (see figure 3.2 (a)).

Therefore, they are mainly in a multidomain state. However, as the milling time increases, the FM particles fracture and become smaller. Thus, many of them reach sizes of around 1 μm (see figure 3.2 (b)). Therefore, after intermediate milling times, a fraction of $SmCo_5$ particles may be in a monodomain state. This can be the reason for the increase of H_C during the first stages of the mechanical milling process (see figure 4.16), although small defects acting as pinning sites could also play some role. However, for longer milling times H_C of $SmCo_5$ milled alone is found to significantly reduce. We have attributed this reduction to the high degree of structural disorder generated in $SmCo_5$ after long-term milling (see for example the small crystallite size and the large microstrains after milling $SmCo_5$ for 32 h in figure 3.15), which may result in a decrease of its magnetic anisotropy and, thus, of its coercivity [7,8]. Nevertheless, H_C of $SmCo_5$ + CoO or $SmCo_5$ + NiO is not found to reduce when the milling time is progressively increased. Actually, in annex 3 (see figures 3.18, 3.20 and 3.21) it has been emphasized that both NiO and CoO slow down $SmCo_5$ structural changes during the milling. This is one of the factors that avoids the H_C reduction after long-term milling.

To check the relationship between $SmCo_5$ structural evolution and H_C, we have plotted in figure 5.1 H_C as a function of $SmCo_5$ crystallite size, $\langle D \rangle_{SmCo5}$, for $SmCo_5$ milled alone, with NiO and with CoO in a weight ratio of 1:1.

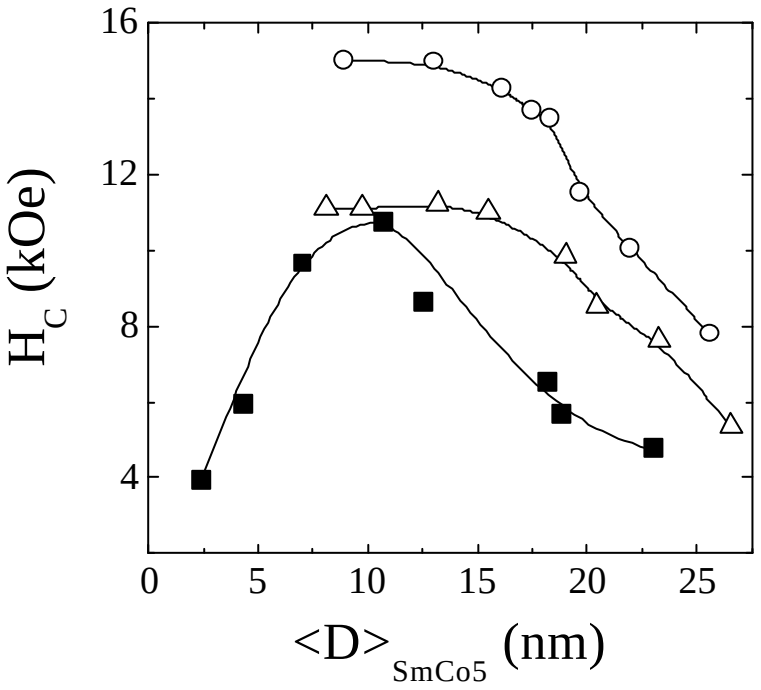

Figure 5.1: Dependence of the coercivity, H_C, on $SmCo_5$ crystallite size, $\langle D \rangle_{SmCo5}$, for $SmCo_5$ milled alone (—■—), with CoO (—Δ—)and NiO (—O—) in the weight ratio 1:1. The lines are a guide to the eye.

It can be seen that, in the three cases, the maximum H_C is obtained for $<D>_{SmCo5}$ of the order of 10-15 nm, much smaller than the single domain size (i.e. d_{Cr} = 0.8 μm) [9], in agreement with other studies dealing with the magnetic properties of ball milled $SmCo_5$ powders [8,10,11]. The figure shows that H_C apparently only reduces for $<D>_{SmCo5}$ lower than 10 nm, which, combined with the large microstrains observed in long-term milled powders (see figure 3.21) indicates that when $SmCo_5$ structure deteriorates the hard magnetic properties of $SmCo_5$ tend to be significantly lost. Therefore, it is not surprising that in $SmCo_5$ + CoO and $SmCo_5$ + NiO milled in the ratio 1:1 H_C remains constant even when the milling time is increased to several hours, since in these two systems $<D>_{SmCo5}$ does not reduce enough, i.e. below 10 nm, even after long-term milling. Moreover, figure 5.1 also shows that for a fixed crystallite sizes, H_C remains higher in $SmCo_5$ + CoO than for $SmCo_5$ milled alone. This behavior can be understood in terms of the role that the PM CoO matrix plays in isolating the different $SmCo_5$ grains. This isolation brings about a decrease of the interparticle FM-FM exchange interactions, which are known to reduce H_C due to the cooperative reversal of several interacting FM particles [12-14]. Nevertheless, the fact that, for a fixed $SmCo_5$ crystallite size, H_C is even higher when it is milled with NiO can be taken as a confirmation that FM-AFM exchange interactions are actually present in the as-milled $SmCo_5$ + NiO powders.

Furthermore, figure 5.2 shows the dependence of H_C on $SmCo_5$ crystallite size, $<D>_{SmCo5}$, for several $SmCo_5$:NiO weight ratios: 1:0, 3:1, 3:2 and 1:1. For all compositions, the maximum H_C is again obtained for $<D>_{SmCo5}$ around 10 – 15 nm. Moreover, in spite of the presence of NiO, H_C is found to decrease for exceedingly small $<D>_{SmCo5}$ values, i.e. after long-term milling of FM with AFM powders in the ratios 1:0, 3:1 and 3:2 (see also figure 4.21). Figure 5.2 also shows that, for a fixed $SmCo_5$ crystallite size, the H_C enhancement is larger for larger AFM contents.

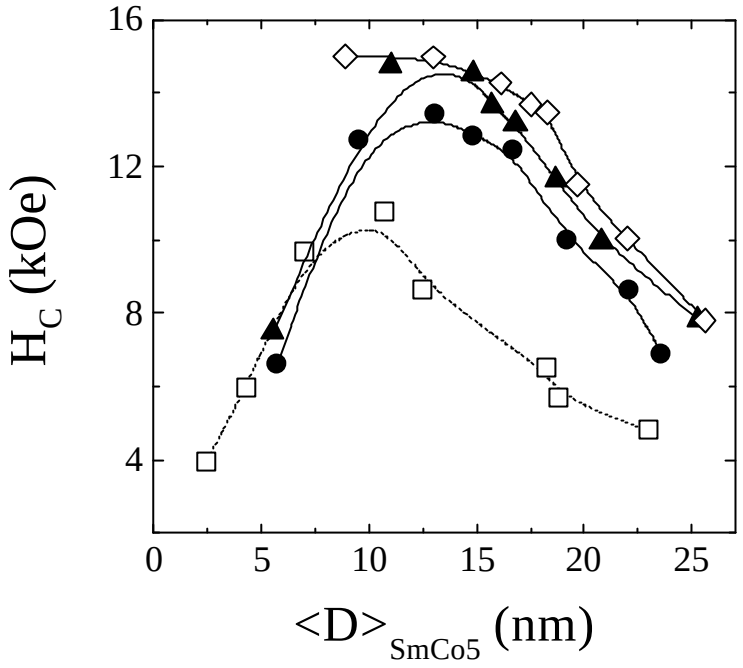

Figure 5.2: Dependence of the coercivity, H_C, on $SmCo_5$ crystallite size, $<D>_{SmCo5}$, for $SmCo_5$ milled with NiO in the weight ratios $SmCo_5$ (1):(0) NiO (-- □ --), $SmCo_5$ (3):(1) NiO (— ● —), $SmCo_5$ (3):(2) NiO (—▲—) and $SmCo_5$ (1):(1) NiO (—◇—). Note that the error bars are smaller than the symbols. The lines are a guide to the eye.

The induction of FM-AFM exchange interactions during the milling implies that, somehow, a process analogous to a field cooling, must take place during the milling. It is well known that, during the milling, due to the impacts between powders and balls, temperature can be locally raised to above the T_N (NiO) (or strictly, to above the blocking temperature, which is always lower than T_N). Actually, Miller et al. have calculated the local temperature rise in a planetary ball mill apparatus to be in excess of 600 K, well above the T_N of NiO (i.e. 590 K) [15]. Since the temperature rise is only effective during a few μs, the local heating may induce some FM-AFM exchange coupling, but may not be enough to drive diffusion processes, which might lead to deterioration of $SmCo_5$ properties. Furthermore, since $SmCo_5$ particles have a large magnetocrystalline anisotropy, they can remain single-domain to very large sizes, i.e. the critical size for single-domain particles in $SmCo_5$ is d_{Cr} = 0.8 μm [9]. Therefore, they can create considerably large microscopic magnetic fields to neighboring NiO grains during the milling. Hence, field cooling could actually be thought to take place during ball milling. This effect can be considered similar to the creation of domains by local flash annealing in FM-AFM bilayers [16]. Figure 5.3 illustrates a possible spin configuration that might be generated in $SmCo_5$ + NiO composites during the milling.

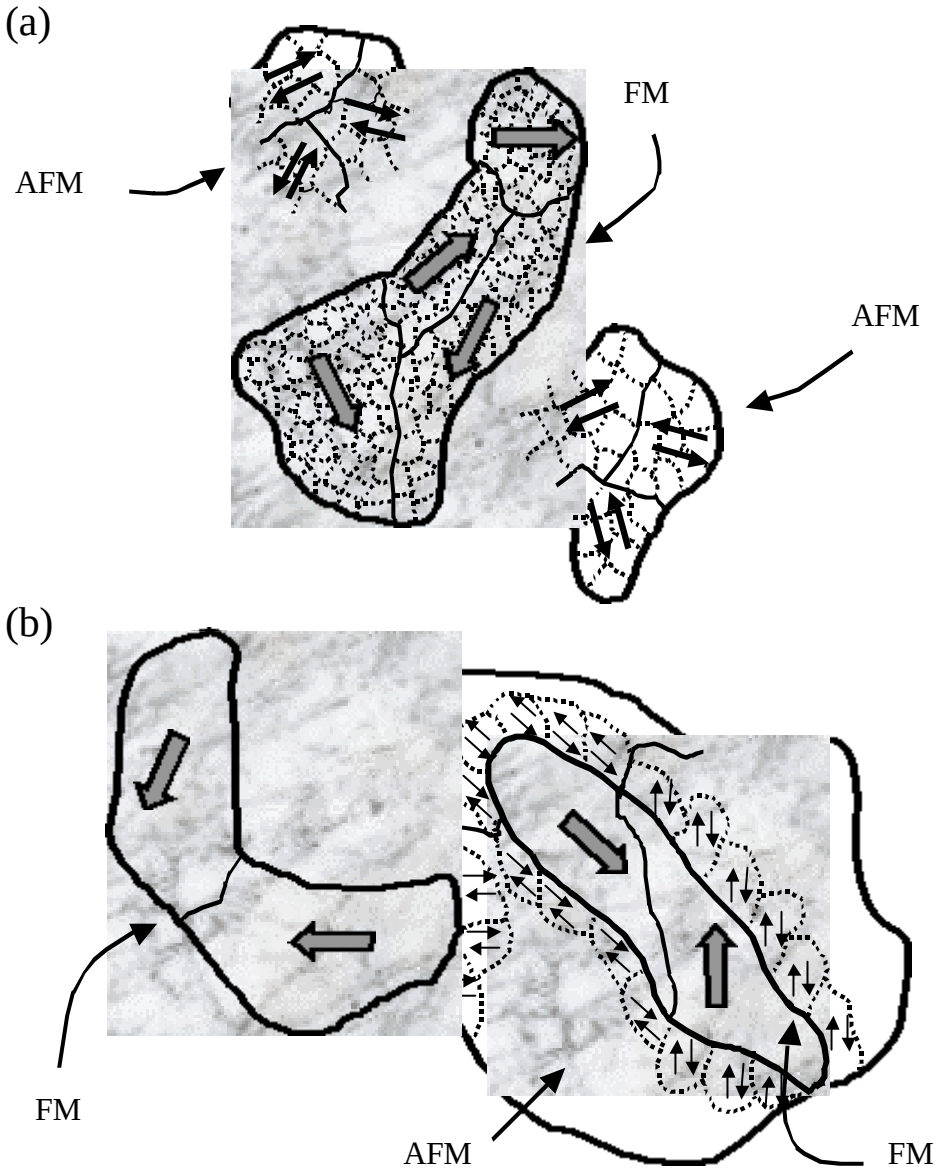

Figure 5.3: Intuitive illustration of the morphology and spin configuration of $SmCo_5$ + NiO powders ball milled together. In (a) the morphology after short-term milling is illustrated, i.e. the FM and AFM particles are still not soldered together. In particular, one FM and two AFM particles are represented, each of them containing a few magnetic domains, which, at the same time, include several crystallites. Note that in (a) the spins in the FM and the AFM do not interact with each other and, consequently, the magnetization directions in the different domains are at random. Fig. (b) represents the morphology generated after long-term milling. In this case, two FM particles have soldered with AFM powders to form one FM-AFM agglomerate. For simplicity, only the crystallites in the AFM located at the interfaces with the FM particles have been represented. The figure shows that, if one assumes that some FM-AFM exchange interactions are induced during the milling, the spins of the AFM grains located near the interfaces with the FM particles will tend to align towards the directions of the neighboring FM domains. This coupling at the interface will result in the local exchange bias effects, i.e. an enhancement of coercivity.

In figure 5.3 (a), which corresponds to $SmCo_5$ milled for short times with NiO, the FM-AFM agglomerates have not been formed yet and, therefore, basically there are no interactions between the FM and AFM grains. Both $SmCo_5$ and NiO particles are so large that they are composed of several crystallites and are in a multidomain state. Since there are no interactions and the powders have not been aligned, their domains remain oriented at random. However, as it is shown in figure 5.3 (b), after long-term milling, when some FM-AFM agglomerates are already created, it is possible that many of the $SmCo_5$ grains embedded in the AFM matrix remain single-domain or just include a few magnetic domains, although they are composed of a large number of small crystallites. This is because the single-domain particle size of $SmCo_5$ is quite large. Therefore, these FM particles can generate reasonable microscopic fields to the neighboring AFM grains, which, during the impacts between powders and balls, may become exchange coupled to the FM. Hence, as shown in the figure, due to FM-AFM exchange interactions, the spins in AFM surrounding the FM particles may become aligned in the magnetization directions of neighboring FM domains. Therefore, as has been described in section 1.3.3, during the hysteresis loop, these AFM spins may exert a microscopic torque to the FM spins, thus resulting in the observed enhancement of H_C [6].

Contrary to $SmCo_5$, the critical size for single-domain behavior in Co is much smaller, e.g. d_{Cr} = 34 nm [9]. Therefore, since the Co particle size, both when milled alone or with NiO, is in the range of a few μm, Co particles remain, in fact, in a multidomain state during the milling. Consequently, the net microscopic magnetic field that each Co particle creates to neighboring NiO grains during the milling is averaged out and becomes much smaller than for $SmCo_5$. Nevertheless, it is worthwhile mentioning that even in Co ball milled with NiO it is possible that some FM-AFM exchange interactions are induced during the milling, i.e. before the field cooling experiments. This can be seen from the results in table 4.1, where already in the as-milled state, H_C is found to be significantly higher for the Co:NiO weight ratios of 3:2 and 1:1 (H_C = 302 and 297 Oe, respectively) than for Co ball milled alone (H_C = 288 Oe).

Nevertheless, essentially no loop shifts are observed in as-milled Co + NiO or $SmCo_5$ + NiO and small loop shifts are only induced in Co + NiO after a field cooling process from above T_N. This is due to the random character of FM-AFM exchange interactions induced during the milling. Namely, in the as-milled state probably each FM particle induces H_E in a different direction and, thus, the effects average out to H_E = 0. Moreover, as has been noted in annex 4, the low magnetic anisotropy of NiO is also partly responsible for the low H_E values observed [6]. However, in spite of the difficulty of directly demonstrating the existence of FM-AFM exchange interactions in as-milled $SmCo_5$ + NiO particles (i.e., as described in the preceding paragraphs, their existence can only be proved indirectly, by comparison with ball milled $SmCo_5$ + CoO powders), we have recently carried out some preliminary torque experiments in oriented $SmCo_5$ + NiO particles, where the obtained curves for $SmCo_5$ + NiO

require the presence of a "*A sin (**q**)*" term in order to be fitted, which is a possible sign of exchange bias effects (see section 1.3.2). Note that by orienting the particles, the randomness of the as-milled powders is reduced, hence allowing the exchange bias effects to be partially observable.

Another remarkable effect that has been observed at room temperature in both Co + NiO and $SmCo_5$ + NiO composites is the enhancement of the squareness ratio. As has been discussed in annex 4, this effect is usually attributed mainly to exchange interactions between FM grains [12-14]. However, our results indicate that also part of this enhancement can be due to FM-AFM exchange interactions. This is a complex effect. However, an intuitive model, depicted in figure 5.4, can be developed to explain, at least qualitatively, how FM-AFM exchange interactions could affect the values of M_R/M_S.

For simplicity, let us assume that the as-milled powders consist of monodomain FM particles, surrounded by polycrystalline AFM shells. If the FM particles were not in a single-domain state, the following interpretation would be similar although only those grains located at the interfaces with the AFM would contribute to the M_R/M_S enhancement. As shown in figure 5.4 (a), at room temperature (i.e. for $T < T_C$), if the applied field is zero and the sample has not been previously magnetized, the spins in the FM grains are oriented along the easy axis of each FM particle. Similarly, for $T < T_N$, the spins in the AFM are oriented along the several AFM easy axes. Therefore, averaging for all particles, the spontaneous magnetization will be approximately zero. If, however, the sample is subsequently heated to $T_C > T_{ANN} > T_N$ and a large enough magnetic field, $H = H_1$, is applied, the spins in the FM will rotate and align towards the direction of the field, while the spins in the AFM will be at random (see fig. 5.4(b)). When the sample is field cooled (applying $H = H_1$) to room temperature, it is likely that, due to the exchange coupling between the FM and the AFM, the spins in the AFM orient in the same direction as those in the FM, i.e. towards the direction of H_1 (see fig. 5.4(c)). Once at room temperature, if the magnetic field is removed, the majority of spins in the FM will orient towards the easy axis of the corresponding FM grain (as in figure 5.4(a)). In addition, due to the coupling with the AFM, some spins in the FM, still remain aligned in the direction of the previous magnetizing field ($H = H_1$), i.e. in the same direction as the spins in the AFM. This would result in an increase of the remanent magnetization as a result of FM-AFM exchange interactions. If the FM particles were multi-domain one would also have to add the effect of FM-FM exchange interactions (e.g. among the several FM crystallites) to FM-AFM exchange interactions, making this intuitive picture increasingly complex. Actually, exchange interactions between soft and hard FM grains are the origin of remanence enhancement in the so-called *spring-magnets* [17,18], as has been described in annex 1.

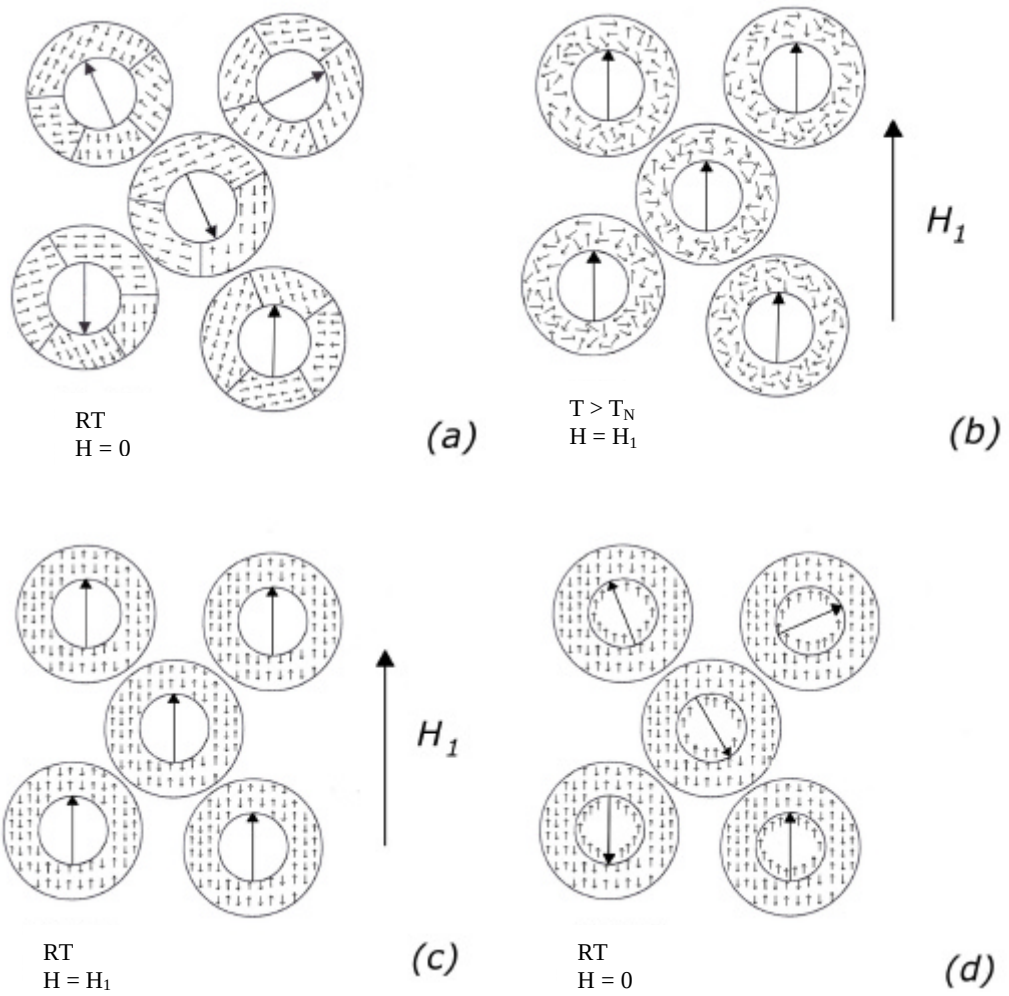

Figure 5.4: Schematic spin configurations used to explain qualitatively the M_R/M_S enhancement due to FM-AFM exchange interactions. In (a) the particles are at room temperature and the applied field is zero. The spins in the FM are oriented along the easy-axis of each FM grain, thus giving an almost zero net magnetization. In the AFM shells the spins are also aligned towards the easy axes. In (b) a large magnetic field ($H = H_1$) is applied at a temperature above T_N but below T_C. As a result the FM spins align with the field (assuming saturation of the FM) while the spins in the AFM are at random since $T > T_N$. In (c) the particles are field cooled ($H = H_1$) to room temperature. If FM-AFM coupling is induced during the cooling, the spins in the AFM will orient in the same direction as the spins in the FM, i.e. along the direction of H_1. Finally, in (d) the field is removed and, therefore, the spins in the FM return to the easy-axes directions. However, if some exchange interactions are present, those spins in the FM located near FM-AFM interfaces can keep aligned in the direction of the previous magnetizing field, thus increasing M_R/M_S.

As is well known, the figure of merit of a hard magnetic material is its maximum energy product, $(BH)_{Max}$, which is roughly proportional to the total area enclosed by the hysteresis loop and is related to the amount of energy that can be stored in the magnet [9,18]. As has been already described in annex 1, large values of the energy product require large coercivities (to make the loop as wide as possible), high saturation magnetizations (to make the loop as long in the *M*-axis as possible) and a squareness ratio close to 1 (to make the loop as square as possible). It has been shown in annex 4 that in ball milled FM-AFM powders both H_C and M_R/M_S can be enhanced due to FM-AFM and FM-FM exchange interactions. Moreover, it has been demonstrated that for AFM contents ranging from 0 to 50 % (weight percent) FM-AFM exchange interactions increase with increasing the AFM content. This is well evidenced in figure 5.5, which shows the dependence of H_E, ΔH_C and $\Delta(BH)_{Max}$ on the FM:AFM ratio for Co ball milled with NiO during the milling times that give maximum ΔH_C, denoted as t_{Max} in annex 4. These curves directly show the effect that FM-AFM exchange interactions have on the improvement of the magnetic properties of the Co-NiO system. For example, it is remarkable that, although the largest values of $(BH)_{Max}$ for Co + NiO are observed for the FM:AFM weight ratio of 3:2 (see fig. 4.10), $\Delta(BH)_{Max}$ (i.e. the enhancement of $(BH)_{Max}$ achieved after the field cooling procedure, which is mainly due to the FM-AFM exchange interactions) is larger for the 1:1 ratio. Actually, the three magnitudes plotted in figure 5.5 reveal that for Co + NiO, FM-AFM exchange interactions are maximum for the 1:1 ratio but they tend to decrease for larger AFM concentrations. This is similar to the dependence of H_C and H_E on the AFM thickness that has been observed in some FM-AFM bilayers, where a decrease of exchange bias effects for large AFM thicknesses has been reported [6,19]. This effect has been attributed to changes in the microstructure or domain structure in the AFM for large thicknesses.

Moreover, as discussed in annex 4, when the AFM content becomes exceedingly high, the maximum energy product of the FM-AFM composites decreases, for both Co + NiO and $SmCo_5$ + NiO [4,20]. This is easily seen in figure 5.6, which summarizes the maximum values of H_C and $(BH)_{Max}$ achieved in the Co-NiO (fig. 5.6 (a)) and $SmCo_5$-NiO (fig. 5.6 (b)) systems after optimization of the FM:AFM ratio and milling time (note that the values plotted are the corresponding to the milling time that gives maximum H_C and $(BH)_{Max}$, respectively, for each composition).

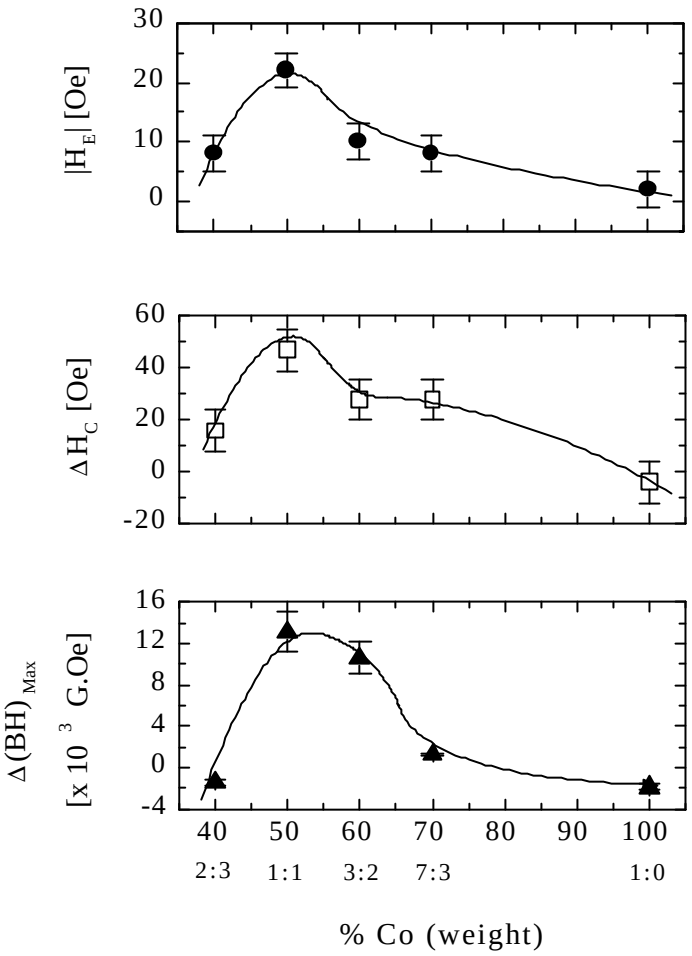

Figure 5.5: Dependence of the loop shift, $|H_E|$, the coercivity enhancement, ΔH_C, and the energy product enhancement, $\Delta(BH)_{Max}$, on the Co weight percentage (FM:AFM weight ratio), for Co ball milled with NiO during times that give maximum values of ΔH_C,. The as-milled powders were annealed at T_{ANN} = 600 K for 0.5 h and field cooled (H = 5 kOe) to room temperature.

This figure summarizes the two-fold role of NiO in the magnetic hardening induced by FM-AFM exchange coupling. As seen in the figure, in both systems, the optimum composition for enhancing H_C is not the same as for increasing $(BH)_{Max}$. This is because, on the one hand, increasing the AFM content mainly brings about an increase of the FM-AFM exchange interactions and, consequently, an increase of H_C and M_R/M_S. However, on the other hand, the presence of the AFM also brings about a reduction of M_S of the composites, since an AFM has a zero net magnetization. As a consequence, a decrease of $(BH)_{Max}$ is observed when the amount of AFM is exceedingly large. Therefore, milling time and composition need to be optimized depending on the desired properties of the magnetic composites.

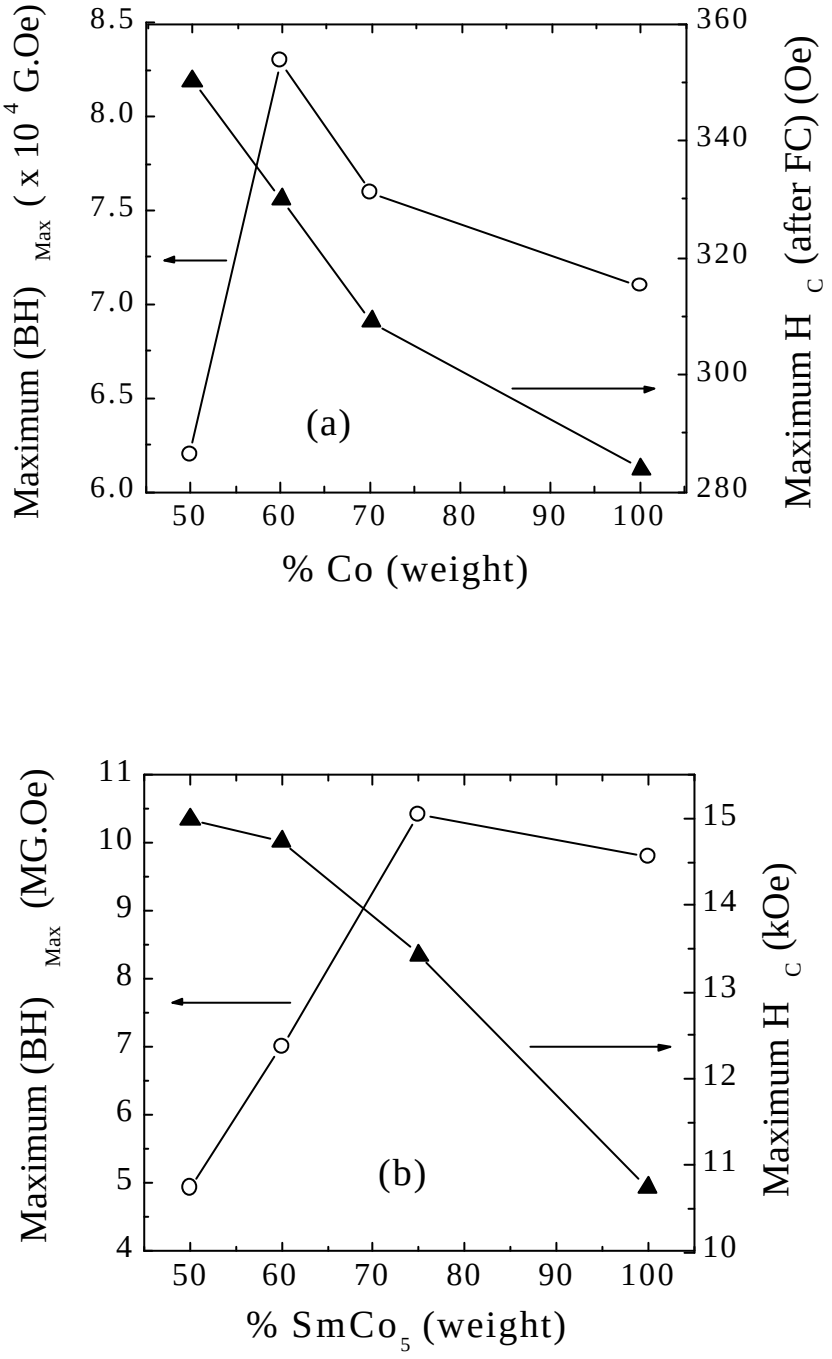

Figure 5.3: (a) Dependence of the coercivity, H_C, and maximum energy product, $(BH)_{Max}$, on the Co weight percentage, after field cooling (FC) the as-milled powders from T_{ANN} = 600 K to room temperature in H = 5 kOe. The values plotted belong to the milling times that give maximum H_C and $(BH)_{Max}$ for each composition. (b) Dependence of the coercivity, H_C, and energy product, $(BH)_{Max}$, on the $SmCo_5$ weight percentage. The values plotted correspond to the milling times that give maximum H_C and $(BH)_{Max}$ for each composition.

Finally, it should be noted that exchange bias effects in bilayers composed of FM-AFM thin films, with very large FM anisotropy (as in the case of $SmCo_5$), have not been studied, neither theoretically or experimentally. Namely, most models dealing with exchange bias considered so far, neglect the role of the FM anisotropy [6,21]. Moreover, there is very little experimental work in which the effect of the FM anisotropy on exchange bias is considered [22]. However, preliminary results from Dr. Zhou's group imply that the coercivity enhancement in FM-AFM bilayers appears to be directly linked with the anisotropy of the FM materials [22].

Therefore, the lack of experimental work in hard magnetic – AFM thin film form and theoretical models taking into account the role of the FM anisotropy, especially in the case of $k_{FM} >> k_{AFM}$, makes the quantitative analysis of our results rather complicated. Moreover, the experimental difficulty in independently controlling crucial parameters affecting exchange bias, such as the AFM and FM particle sizes, interface roughness or the FM and AFM domain structures, also results in the complexity of the interpretation of our results.

References

[1] J. Sort, J. Nogués, X. Amils, S. Suriñach, J.S. Muñoz, M.D. Baró, Mat. Sci. Forum **343-346** (2000) 812.

[2] J. Sort, J. Nogués, X. Amils, S. Suriñach, J.S. Muñoz, M.D. Baró, Mat. Res. Soc. Symp. Proc. **581** (2000) 641.

[3] J. Sort, J. Nogués, S. Suriñach, J.S. Muñoz, E. Chappel, F. Dupont, G. Chouteau, M.D. Baró, Mat. Sci. Forum **386-388** (2002) 465.

[4] J. Sort, S. Suriñach, J.S. Muñoz, M.D. Baró, J. Nogués, G. Chouteau, V. Skumryev, G.C. Hadjipanayis, Phys. Rev. B **65** (2002) 174420.

[5] J. Sort, J. Nogués, S. Suriñach, J.S. Muñoz, M.D. Baró, E. Chappel, F. Dupont, G. Chouteau, Appl. Phys. Lett. **79** (2001) 1142.

[6] J. Nogués, I. K. Schuller, J. Magn. Magn. Mater. **192** (1999) 203.

[7] K. J. Strnat and R. M. W. Strnat, J. Magn. Magn. Mater. **100** (1991) 38.

[8] D. L. Leslie-Pelecky, E. M. Kirkpatrick, and R. L. Schalek, Nanostruct. Mater. **12** (1999) 887; D. L. Leslie-Pelecky and R. L. Schalek, Phys. Rev. B **59** (1999) 457.

[9] R. Skomski, J. M. D. Coey, *Permanent Magnetism* (Institute of Physics Publishing, Bristol, 1999).

[10] A. Y. Yermakov, V. V. Serikov, V. A. Barinov, Y. S. Shur, Fiz. Met. Metalloved. **42** (1976) 408.

[11] Z. Chen, X. Meng-Burany, G. C. Hadjipanayis, Appl. Phys. Lett. **75** (1999) 3165.

[12] A. Hernando, I. Navarro, J. M. González, Europhys. Lett. **20** (1992) 175.

[13] W. Rave, K. Ramstöck, J. Magn. Magn. Mater. **171** (1997) 69.

[14] T. Schrefl, J. Fidler, H. Kronmüller, Phys. Rev. B **49** (1994) 6100; T. Schrefl, H. F. Schmidts, J. Fidler, H. Kronmüller, J. Magn. Magn. Mater. **124** (1993) 21; R. Fischer, T. Schrefl, H. Kronmüller, J. Fidler, J. Magn. Magn. Mater. **153** (1996) 35.

[15] P. J. Miller, C. S. Coffey, V. F. Devost, J. Appl. Phys. **59** (1986) 913.

[16] N. M. Salanskii, V. A. Serëdkin, V. A. Burmakin, A. V. Nabatov, Sov. Phys. JEPT **38** (1974) 1011.

[17] E.F. Kneller, R. Hawig, IEEE Trans. Magn. **27** (1991) 3588.

[18] G.C. Hadjipanayis, J. Magn. Magn. Mater. **200** (1999) 373.

[19] C. Tsang, N. Heiman, K. Lee, J. Appl. Phys. **52** (1981) 2471; K. T. Y. Kung, L. K. Louie, J. Appl. Phys. **69** (1991) 5634; R. Jungblut, R. Coehoorn, M. T. Johnson, J. aan de Stegge, A. Reinders, J. Appl. Phys. **75** (1994) 6659.

[20] J. Sort, J. Nogués, X. Amils, S. Suriñach, J.S. Muñoz, M.D. Baró, J. Magn. Magn. Mater. **219** (2000) 53.

[21] R. L. Stamps, J. Phys. D: Appl. Phys. **33** (2000) R247.

[22] L. Wang, B. You, S. J. Yuan, J. Du, W. Q. Zou, A. Hu, S. M. Zhou *(private communication)*.